Study of Ligand−Receptor Interactions by Fluorescence Correlation Spectroscopy with Different Fluorophores: Evidence That the Homopentameric 5-Hydroxytryptamine Type 3_{As} Receptor Binds Only One Ligand†

T. Wohland, K. Friedrich, R. Hovius, and H. Vogel*

Laboratory of Physical Chemistry of Polymers and Membranes, Chemistry Department, Swiss Federal Institute of Technology, CH-1015 Lausanne, Switzerland

Received February 15, 1999; Revised Manuscript Received April 29, 1999

ABSTRACT: The 5-hydroxytryptamine receptor of type 3 was investigated by fluorescence correlation spectroscopy (FCS). Binding constants of fluorescently labeled ligands, the stoichiometry, and the mass of the receptor are readily accessible by this technique, while the duration of measurement is on the order of seconds to minutes. The receptor antagonist 1,2,3,9-tetrahydro-3-[(5-methyl-1*H*-imidazol-4-yl)methyl]-9-(3-aminopropyl)-4*H*-carbazol-4-one (GR-H) was labeled with the fluorophores rhodamine 6G, fluorescein, *N*-[7-nitrobenz-2-oxa-1,3-diazol-4-yl], and the cyanine dye Cy5. These labels cover a large part of the visible electromagnetic spectrum. It is shown that the photophysical and chemical properties have a direct influence on the measurement quality (duration of measurement, signal-to-noise ratio) and the ligand−receptor interactions (dissociation constants), respectively. This makes it necessary to choose a suitable label or a combination of labels for receptor studies. The affinities of the fluorescently labeled ligands determined by FCS were virtually identical to the values obtained by radioligand binding experiments. Moreover, the dissociation constant of a nonfluorescent receptor ligand was determined successfully by an FCS competition assay. The experimental results showed that only one antagonist binds to the receptor, in agreement with measurements previously published [Tairi et al. (1998) *Biochemistry 37*, 15850−15864].

Fluorescence correlation spectroscopy (FCS)[1] measures statistical fluctuations of the fluorescence intensity in a small illuminated sample volume to obtain information about the chemical and photophysical properties of individual fluorescent molecules. This technique was first described more than two decades ago *(1−4)* and has recently regained interest for the investigation of and screening for molecular properties and interactions *(5−10)*. Since then, several ligand−receptor systems have been investigated *(11, 12)*, but so far no systematic comparative studies have been conducted on how a particular type of fluorophore influences the FCS measurement itself or the reactions between the interacting molecules. However, because FCS requires suitable fluorophores that, with a few exceptions, are extrinsic labels, it is essential to select a fluorescent probe that allows accurate measurements without disturbing the interaction between the molecules under investigation.

In the present communication we investigate the specific interaction between fluorescently labeled ligands and the short spliced form of the purified serotonin (=hydroxytryptamine) type 3A receptor ($5HT_{3As}$ receptor). This receptor is a typical example of a neuroreceptor functioning as a ligand-gated ion channel. Membrane receptors, in particular channel proteins, are important targets for therapeutic agents *(13)*. In this respect, the investigation of ligand−receptor interactions is equally important for fundamental and applied research. It provides necessary information on the molecular mechanism of receptor function and, in addition, is the basis for the screening of potential pharmaceutical active compounds. FCS promises, in this context, novel opportunities with respect to sensitivity, miniaturization, and testing large numbers of ligands or receptors.

The $5HT_{3As}$ receptor is ideally suited to investigate the applicability of this analytical technique in the field of neuroreceptors. First, this receptor is of medical interest as a target of several important therapeutic agents. Such compounds have an influence, for instance, on depression,

† This work was financially supported by the Swiss National Science Foundation Priority Program for Biotechnology, Project 5002-35180 (H.V.).

* Address correspondence to this author at DC-LCPPM, EPFL, CH-1015 Lausanne, Switzerland. Phone +41-21-693-3155; Fax +41-21-693-6190; E-mail Horst.Vogel@epfl.ch.

[1] Abbreviations: FCS, fluorescence correlation spectroscopy; ACF, autocorrelation function; ACT, average correlation time; $5HT_{3As}$ receptor, short splice form of the mouse 5-hydroxytryptamine receptor of type 3A; GR-H, GR119566X, or 1,2,3,9-tetrahydro-3-[(5-methyl-1*H*-imidazol-4-yl)methyl]-9-(3-aminopropyl)-4*H*-carbazol-4-one; GR−Flu, GR186741X, or 1,2,3,9-tetrahydro-3-[(5-methyl-1*H*-imidazol-4-yl)methyl]-9-[3-amino-[*N*-(fluorescien)thiocarbamoyl]propyl]-4*H*-carbazol-4-one; GR−NBD, 1,2,3,9-tetrahydro-3-[(5-methyl-1*H*-imidazol-4-yl)methyl]-9-(3-amino-(*N*-[7-nitrobenz-2-oxa-1,3-diazol-4-yl])propyl)-4*H*-carbazol-4-one; GR−Rho, 1,2,3,9-tetrahydro-3-[(5-methyl-1*H*-imidazol-4-yl)methyl]-9-[3-amino-[*N*-(rhodamime B)thiocarbamoyl]-propyl]-4*H*-carbazol-4-one; GR−Cy5, 1,2,3,9-tetrahydro-3-[(5-methyl-1*H*-imidazol-4-yl)methyl]-9-[3-amino-[*N*-(Cy5)amido]propyl]-4*H*-carbazol-4-one; [^{3}H]GR65630, 3-(5-methyl-1*H*-imidazol-4-yl)-1-(1-[^{3}H]-methyl-1*H*-indol-3-yl)propanone; biotin−fluorescein, 5-[*N*-[5-[*N*-[6-(biotinoylamino)hexanoyl]amino]pentyl]thioureidyl]fluorescein; $C_{12}E_9$, nonaethyleneglycol monododecyl ether; mCPBG, 1-(*m*-chlorophenyl)-biguanide; PBG, phenylbiguanide; Rho 6G, rhodamine 6G; NBD, *N*-[7-nitrobenz-2-oxa-1,3-diazol-4-yl]; HEPES, 4-(2-hydroxyethyl)piperazine-1-ethanesulfonic acid; nACh receptor, nicotinic acetylcholine receptor.

10.1021/bi990366s CCC: $18.00
Published on Web 06/15/1999

Table 1: Properties of the Fluorophores

	M_w[a] (Da)	Abs_{max}[b]	Em_{max}[c]	ϵ[d] (M^{-1} cm^{-1})	QY[e]
NBD	183	465	535	8000	0.3−0.75
fluorescein	389	494	518	80000	0.19−0.74
Rho 6G	479	528	551	100000	0.98
R18	731	556	578	125000	0.31−0.49
Cy5	791	649	670	250000	>0.28

[a] M_w is the relative molecular mass. [b] Abs_{max} is the wavelength of maximal absorption. [c] Em_{max} is the wavelength of maximal fluorescence emission. [d] ϵ is the molar extinction coefficient. [e] QY is the quantum yield.

anxiety, and migraine. Antagonists of the receptor prevent nausea and emesis in cancer patients undergoing chemotherapy or radiotherapy *(14)*. Second, the interaction between the receptor and several suitably labeled ligands can be studied with high sensitivity by fluorescence detection *(15, 16)*.

In the case of the $5HT_{3As}$ receptor the functional channel is assumed to be composed of five identical protein subunits, each with a relative molecular mass of 54−65 kDa *(16)*. There are structural similarities to other ligand-gated ion channels such as the nicotinic acetylcholine receptor (nACh receptor) and the $GABA_A$ receptor *(17)*. The homopentameric structure of the $5HT_{3As}$ receptor implies the existence of five putative binding sites for ligands, but up to now the number of ligands binding to the receptor has not been determined unequivocally (see references in *16*). Experiments presented in the literature suggest that 1−3 agonist molecules have to bind to open the channel, that desensitization is caused by 4−5 bound agonists, and that at least one antagonist has to bind to inhibit channel activation. However, recently it was shown theoretically *(18)* that a protein consisting of five identical subunits cannot have a Hill coefficient of less than 1.3. An important goal of this work is to obtain by concentration measurements with FCS an independent and direct determination of the stoichiometry of ligand binding. Recently an additional subunit, the $5HT_{3B}$ receptor subunit, has been discovered with a different primary sequence and pharmacology *(19)*.

Here, we concentrated on the interaction of the $5HT_{3As}$ receptor with the antagonist 1,2,3,9-tetrahydro-3-[(5-methyl-1*H*-imidazol-4-yl)methyl]-9-(3-aminopropyl)-4*H*-carbazol-4-one (GR-119566X = GR-H), which was labeled with one of four different fluorophores (Table 1). It was investigated how the different photophysical characteristics of these fluorophores, which are representative for a wide range of labels, influence the results obtained by FCS and how the different molecular properties of these fluorophores disturb the molecular interaction between the ligand and its receptor.

We show that with FCS experiments the molecular mass of the $5HT_{3As}$ receptor, the equilibrium constant of the ligand binding reaction, and the corresponding stoichiometry can be measured. Moreover competition studies with nonfluorescent competitors can be performed when the equilibrium constant for the fluorescently labeled ligand has been measured. However, the accuracy of the measurements is strongly influenced by the choice of fluorophore and is limited by intrinsic properties of the FCS technology.

First, the antagonist GR-119566X labeled with fluorescein (GR−Flu) was studied. The binding of this ligand to the purified $5HT_{3As}$ receptor has recently been characterized in detail by radioligand binding and steady-state fluorescence assays *(15, 16)*. The pharmacophore was then labeled with the following fluorophores: *N*-[7-nitrobenz-2-oxa-1,3-diazol-4-yl] (NBD), rhodamine 6G (Rho 6G), and the cyanine dye Cy5. This allows a direct comparison of the different binding characteristics of the labeled ligands and therefore an examination of the influence of the fluorophores on binding. In the following we refer to these ligands as GR−NBD, GR−Rho, and GR−Cy5.

With the combination of these fluorophores, the binding constants and the stoichiometry of ligand binding can be measured accurately, and the relative molecular mass of the receptor can be estimated.

THEORY

FCS. In a FCS experiment fluctuations of the fluorescence $\partial F(t)$ around the average fluorescence $\langle F \rangle$ are measured, yielding information on molecular processes or molecular motions. The fluctuations of the fluorescence signal stem from changes in either the number of fluorescent particles or the fluorescence quantum yield of the particles in the open probe volume, which is defined by the focal volume of a tightly focused laser beam. To analyze these fluctuations the autocorrelation function (ACF) of the fluorescence intensity is calculated by

$$G(\tau) = \frac{\langle F(0)F(\tau)\rangle}{\langle F(\tau)\rangle^2} \quad (1)$$

The angular brackets $\langle\rangle$ indicate a time average, F is the fluorescence signal as a function of time, and τ is the correlation time.

In our FCS experiments, the fluorophores are excited by a laser beam with a Gaussian beam profile and the emitted fluorescence is observed through a pinhole. Under these conditions the probe volume can be described by a Gaussian distribution in all three Cartesian coordinate axes. ω_1 is defined as the distance from the optical axis and ω_2 as the distance in the z-direction at which the laser intensity has dropped by $1/e^2$, and K is defined as $K = \omega_{2/}\omega_1$.

If only translational diffusion is observed, the ACF is given by *(20, 21)*

$$G(\tau) = \frac{1}{\gamma N}\left(1 + \frac{\tau}{\tau_D}\right)^{-1}\left(1 + \frac{\tau}{K^2\tau_D}\right)^{-1/2} + G_\infty = \frac{1}{\gamma N} g_{3d}(\tau) + G_\infty \quad (2)$$

The correlation or diffusion time τ_D is defined as

$$\tau_D = \frac{{\omega_1}^2}{4D} \quad (3)$$

D is the diffusion coefficient, and N is the average number of light emitting particles diffusing in the focal sample volume. γ is a correction factor considering the intensity profile in the focus; $\gamma = \sqrt{8}$ for a Gaussian intensity profile in three dimensions *(8)*. This factor γ is omitted in the following equations as it does not influence the other fit parameters. It should, however, be reconsidered if absolute concentrations are to be calculated from FCS measurements. G_∞ is the limiting value of $G(\tau)$ for $\tau \rightarrow \infty$, which is in

general 1. $g_{3d}(\tau)$ is the ACF of one particle for three-dimensional diffusion. The free parameters for a fit are N, K, G_∞, and τ_D. The parameter K describes the shape of the probe volume, which is determined by the size of the laser focus and the pinhole. As a consequence, K should not change if the size of the focus and the pinhole are kept constant.

At higher laser intensities, a triplet state of the chromophore can be excited. As described elsewhere *(22, 23)*, this leads to

$$G(\tau) = \frac{1}{N'} g_{3d}(\tau)[F_{trip} e^{\tau/\tau_{trip}} + (1 - F_{trip})] + G_\infty \quad (4)$$

F_{trip} is the mole fraction of dye molecules in the triplet state, τ_{trip} is the lifetime of the triplet state, and $N' = N(1 - F_{trip})$.

If several components are present, the model has to be extended. Taking into account different quantum yields for the general case of R components, we obtain *(8)*

$$G(\tau) = [\sum_{i=1}^{R} \alpha_i^2 \langle N_i \rangle g_{3di}(\tau)]/[\sum_{i=1}^{R} \alpha_i \langle N_i \rangle]^2 + G_\infty \quad (5)$$

and

$$g_{3di}(\tau) = (1 + 4D_i\tau/{\omega_1}^2)^{-1}(1 + D_i\tau/K^2{\omega_1}^2)^{-1/2} \quad (6)$$

$\alpha_i = Q_i/Q_1$, where the fluorescence yield Q_i of a particle is defined as a product of absorbance, fluorescence quantum efficiency, and experimental fluorescence collection efficiency of the ith species. When $R = 1$, eq 5 reduces to eq 2. To include a triplet state for a component, the functions $g_{3di}(\tau)$ in eq 5 have to be changed according to eq 4.

DIFFUSION

Here only the relations between the diffusion coefficient D, the mass of the diffusing molecule, and the correlation time measured by FCS will be considered. For a more comprehensive description of the molecular theory of diffusion see ref *24*. The translational diffusion coefficient of a particle in a viscous medium is given by the Stokes−Einstein equation (e.g., ref *25*)

$$D = \frac{kT}{f} \quad (7)$$

k is the Boltzmann constant, T is the temperature, and f is the friction coefficient. For the simplest case of a spherical particle the friction coefficient is given by

$$f = 6\pi\eta r \quad (8)$$

with the viscosity of the solvent η and the radius of the sphere r. The mass of a sphere is given by

$$M = \rho V = \frac{3}{4}\pi r^3 \rho \quad (9)$$

where ρ is the mass density of the sphere, V is its volume, and r is its radius. Therefore the diffusion coefficient is inversely proportional to the cubic root of the mass

$$D \sim M^{-1/3} \quad (10)$$

and the correlation time proportional to the cubic root of the mass

$$\tau_D \sim M^{1/3} \quad (11)$$

The approximation of molecules as hard spheres is reasonable for compact molecules. By use of eqs 10 and 11, all diffusion coefficients can be determined if the setup is calibrated on the basis of one standard molecule, which in our case is Rho 6G [$D = 2.8 \times 10^{-6}$ cm^2 s^{-1} *(21)*]. All other diffusion coefficients follow from

$$D_x = \frac{\tau_{Rho}}{\tau_x} D_{Rho} \quad (12)$$

D_{Rho} is the diffusion coefficient and τ_{Rho} is the correlation time of Rho 6G, and D_x and τ_x are the diffusion coefficient and correlation time for the molecule to be measured.

MATERIALS AND METHODS

Chemicals. The radioligand 3-(5-methyl-1*H*-imidazol-4-yl)-1-(1-[^{3}H]methyl-1*H*-indol-3-yl)-propanone ([^{3}H]GR65630; 61 Ci/mmol) was from NEN-DuPont (Boston, MA). The antagonists granisetron, GR-H, and the fluorescent ligand GR−Flu were obtained from the former Geneva Biomedical Research Institute (Glaxo Wellcome, Geneva, Switzerland). The agonist quipazine was from Tocris-Cookson (Langford, U.K.). Monododecyl nona(ethylene glycol) ($C_{12}E_9$) was from Fluka (Buchs, Switzerland). The reactive fluorophores were monofunctional Cy5 succinimide (Amersham, Zürich, Switzerland), rhodamine 6G isothiocyanate, NBD fluoride (both Fluka, Buchs, Switzerland), and fluorescein 5-isothiocyanate (Molecular Probes, Eugene, OR). Carboxyfluoresecein, octadecylrhodamine B chloride (R18), 5-[*N*-[5-[*N*-[6-(biotinoylamino)hexanoyl]amino]pentyl]thioureidyl]fluorescein (biotin−fluorescein), and streptavidin were from Molecular Probes.

All other products used were of the highest quality available and purchased from regular sources.

Preparation of the Fluorescent Ligands. GR-H was labeled with four different fluorescent labels by reacting it with activated fluorophores in the presence of a base (triethylamine or diisopropylethylamine) in dimethylformamide−dimethyl sulfoxide mixtures for 3−16 h at room temperature. The fluorescently labeled ligands were purified by chromatography on silica gel G60 (Merck, Darmstadt, Germany). Purity of the products was confirmed by high-pressure liquid chromatography using a gradient changing from water with 0.2% 1,1,1-trifluoroacetic acid to acetonitrile/2-propanol (1/1) with 0.2% 1,1,1-trifluoroacetic acid on a Nucleosil 100-7 C_2 column (125 × 4 mm^2, Machery-Nagel, Düren, Germany).

Buffers. Buffer 1 was composed of 10 mM 4-(2-hydroxyethyl)piperazine-1-ethanesulfonic acid (HEPES) and buffer 2 of 10 mM HEPES and 0.4 mM $C_{12}E_9$. Both buffers were adjusted to pH = 7.4.

Preparation of Solubilized 5HT$_{3As}$ Receptor. A 5HT$_{3As}$ receptor carrying a C-terminal hexahistidine tag was expressed in baby hamster kidney cells using Semliki Forest virus vectors *(26)*. For purification, a suspension of cell membranes was solubilized in $C_{12}E_9$ and the receptor was purified in one step by immobilized metal-ion chromatog-

raphy as described in detail elsewhere *(27)*. The buffer of the receptor preparation was then exchanged for buffer 2 by gel filtration (G-25 Sephadex column, NAP-10, Pharmacia, Uppsala, Sweden). The preparation was stored at −80 °C until further use.

FCS Instrumentation. FCS measurements were performed with a home-built instrument using an inverted microscope (Axiovert 100 TV, Carl Zeiss AG, Oberkochen, Germany) as a central part.

The 488 and 514 nm lines of an Ar^+ laser with an output beamwaist of 3 mm (Coherent Inc., Santa Clara, CA) were used for the excitation of NBD, fluorescein, and Rho 6G. Cy5 was excited at 633 nm with a helium−neon (HeNe) laser (Melles Griot, Irvine, CA) with a beamwaist of 1 mm.

The laser beam output width was increased by a factor of 2 (Ar^+ laser) or 3 (HeNe laser) by use of a Keplerian beam expansion. It was then reflected by a dichroic mirror (for Flu and NBD, FT510, Carl Zeiss; for Rho, FT540; and for Cy5, 645DRLP02, Omega, Brattleboro, VT) and coupled into the microscope. The beam expansion ensured that the back aperture of the microscope objective (63x C-Apochromat, NA 1.2, water immersion with cover slip correction for a thickness between 0.16 and 0.18 μm, Carl Zeiss) was fully illuminated, thus providing a tightly focused laser beam. The fluorescence signal of the sample was collected with the same objective and passed a band-pass filter (for Flu and NBD, BP515−565, Carl Zeiss; for Rho, 565DF72; and for Cy5, 670DF40, Omega) to reduce the background signal. A pinhole (50 μm diameter) was installed in an image plane of the microscope to discriminate against out-of-focus signals. The collected fluorescence light was then focused onto an avalanche photodiode [SPCM-100 (EG&G), Precitek Electronic AG, Langnau, Switzerland]. The electrical signal was fed into a hardware correlator (ALV-5000, ALV-GmbH, Langen, Germany) and the ACFs were calculated by use of a semilogarithmic time scale.

The power of the laser beam entering the microscope was set to 60−80 μW for the Ar^+ laser and to 7 mW for the HeNe laser. Such power levels created sufficiently high fluorescence signals per molecule but were still low enough to keep photobleaching negligible. The actual power in the focal volume was lower due to losses at lenses, beam splitter, and dichroic mirror. The laser light intensity in the focal volume was not measured.

The beamwaist radius of the focused Ar^+ laser beam was determined to be approximately 0.25 μm for the wavelengths of 488 and 514 nm by measuring the translational diffusion of Rho 6G in water, assuming a diffusion coefficient of $D = 2.8 \times 10^{-6}$ cm^2 s^{-1} *(21)*. For the HeNe laser with a wavelength of 633 nm the beam waist is estimated to be 0.32 μm by use of Gaussian optics *(28)*.

FCS Experiments. For the calibration measurements with NBD, fluorescein, Rho 6G, Cy5, and the fluorescently labeled ligands, a droplet of 50 μL of the sample solution was placed on a glass cover slide on the microscope table.

Ligand−receptor binding experiments were performed according to two different procedures: For GR−Flu, GR−NBD, and GR−Rho, a 50 μL droplet of the ligand in buffer 2 was first deposited on a cover slide and the receptor was then titrated from a stock solution to this droplet in amounts between 1 and 5 μL. Binding of the ligands occurred almost instantaneously (delay between the addition of receptor and the start of the measurement was about 30 s) and no change in binding was observed for longer times. This procedure is especially well suited for Rho 6G-labeled ligands because a depletion of these ligands from the solution could be observed for longer times due to unspecific interactions between the cover slide and the fluorophore. For the binding studies with GR−Cy5 a separate sample was prepared for each receptor concentration. The sample solutions were prepared at least 1 h before the measurements to ensure that equilibrium had been reached. A 50 μL droplet of the corresponding sample was then placed on a cover slide just before the measurement.

The center of the focus of the laser beam was in the droplet 50 μm above the cover slide. For every experiment 10 independent measurements were performed. The measuring time was 60 s for NBD, fluorescein, and Rho 6G and 30 s for Cy5. The background signal in water and in the particular buffers was less than 0.2 kHz, while the signal of the probe molecules was usually between 2 and 110 kHz, depending on the fluorophore and its concentration.

The setup was calibrated with Rho 6G (514 nm), carboxyfluorescein (488 nm), and Cy5 (633 nm). All other experiments were based on these calibrations. The diffusion time and thus the average size of the $C_{12}E_9$ micelles in buffer 2 was determined by adding R18, which was incorporated almost completely into the detergent micelles. For the binding experiments, we measured the ligand first in buffer 1 to determine its diffusion time τ_D and then in buffer 2 to determine if the ligand partitioned into micelles. Knowing the diffusion time of the ligand in solution, the diffusion time of the ligand-containing micelles can be determined and be compared to the calibration measurements with R18. To verify that the measured ligand binding is specific, the receptor was preincubated with 10 μM quipazine for at least 1 h before addition to the fluorescently labeled ligands, and binding was measured again. At this concentration quipazine is known to completely inhibit the receptor binding of GR-H and GR-Flu *(16)*.

The affinity of the nonfluorescent antagonist granisetron for the $5HT_{3As}$ receptor was determined by competition experiments. Solutions of constant total ligand and receptor concentrations but with varying competitor concentrations were prepared at least 1 h before measurement. Aliquots (50 μL) of these solutions were then deposited on a cover slide and the ACFs were measured.

Evaluation of the experimental ACFs was performed in order of increasing complexity, using parameters obtained from less complex systems. All experimental ACFs were first fitted by a one-component model (eq 4), including a possible triplet state. With this method one monitors the average correlation time (ACT) of the fluorescent molecules in solution. Shifts of the ACT to longer values indicate that at least a fraction of the fluorescent molecules diffuse more slowly, reflecting an increase in mass due to the binding to other components *(12)*. The ACFs for the ligands measured in buffer 2 were fitted with a two-component model (eq 5 with $R = 2$), considering free ligands and ligands incorporated into micelles, including a triplet state if necessary, while keeping as fixed parameter the above determined correlation time of the free ligand in buffer 1. The ACFs for the ligand−receptor solutions were evaluated with a three-component model (eq 5 with $R = 3$) if the ACT indicated that ligand

was bound or that the fraction of bound ligand increased upon addition of receptor. The diffusion times (τ_D) from the previous measurements (ligand in solution, ligand in micelles) were held fixed in this model. The three-component model takes account of the ligand receptor complex and includes a possible triplet state.

Fitting of Models to the FCS Data. The appropriate model is fitted with a least-squares fit (Levenberg−Marquardt method). This method gives usually good results for the fit but is not strictly appropriate for photon statistics. The least-squares method is applicable for variables with a Gaussian probability distribution. Photon statistics, however, follow a Poisson distribution. Nonetheless, this method is commonly used and gives reasonable results. In such a fit χ^2 is defined as

$$\chi^2 = \sum\left(\frac{y - y_i}{\sigma_i}\right)^2 \tag{13}$$

where y is a particular value of the fit function, y_i is an experimental data value, and σ_i is the estimated standard deviation of the measurement. For comparison of the goodness of the fits the reduced values are calculated as $\chi_\nu^2 = \chi^2/(n - p)$ with n as the number of points and p as the free parameters in the fit. The standard deviation for photon correlation measurements was calculated by Koppel *(29)* and corrected by a factor of N^4 to compensate for the normalization of our correlator:

$$\sigma^2(G(\tau)) = \frac{1}{M}\frac{1}{N^2}\left\{\frac{(1 + g^2(\Delta\tau))(1 + g^2(\tau))}{1 - g^2(\Delta\tau)} + 2m\, g^2(\tau)\right\} \tag{14}$$

One has to be aware of the fact that in our experiments the values for χ_ν^2 are usually smaller than unity for a good fit ($0.4 < \chi_\nu^2 < 0.8$). This indicates that the standard deviation estimated by the equation of Koppel is too high *(21)*. According to theory $\chi_\nu^2 = 1$ for a perfect fit; i.e., the standard deviation of the measurement and the deviation of the fitted function from the data are of the same order of magnitude. Nevertheless, the absolute value of χ_ν^2 and its change for different models can give an indication if a model is adequate and which of the models is most likely to represent the physical reality *(30)*.

Models for Data Treatment. As will be shown in the Results section, the number of fluorescent particles remains constant upon the addition of $5HT_{3As}$ receptor to a solution of fluorescently labeled ligands. Under this condition, the interaction between the corresponding ligand and receptor can be described by a 1:1 stoichiometry: R + L ⇔ RL. R represents the receptor, L the ligand, and RL the receptor ligand complex. For the binding studies we can express the number of bound fluorescent ligands in eq 5 as the fraction of all fluorescent ligands in solution:

$$y = \frac{[RL]}{[L]_t} \tag{15}$$

$[L]_t$ represents the total ligand concentration and [RL] is the concentration of the ligand−receptor complex. Denoting the concentration of the free ligand as [L], the total receptor concentration as $[R]_t$, and the free receptor concentration as [R], one can show that with the following definition of the dissociation constant K_d

$$K_d = \frac{[R][L]}{[RL]} = \frac{([R]_t - [RL])([L]_t - [RL])}{[RL]} = [L]_t y - [L]_t + \frac{[R]_t}{y} - [R]_t \tag{16}$$

y can be expressed as

$$y = \frac{(K_d + [L]_t + [R]_t)}{2[L]_t} - \left(\frac{(K_d + [L]_t + [R]_t)^2}{4[L]_t^2} - \frac{[R]_t}{[L]_t}\right)^{1/2} \tag{17}$$

For all binding studies we fitted this function by a least-squares method to the data, and thus determined the corresponding dissociation constants K_d. Because of the titration of the receptor to the ligand, $[R]_t$ and $[L]_t$ change simultaneously at each titration step for GR−NBD, GR−Flu, and GR−Rho. For GR−Cy5, $[L]_t$ was kept constant for all preparations, and only the amount of receptor $[R]_t$ changes from sample to sample. Therefore we chose to display the percentage of fluorescently labeled ligand bound to the receptor y as a function of $[R]_t/[L]_t$.

Binding inhibition curves were fitted to

$$y = \frac{y_0}{1 + (IC_{50}/[\text{competitor}])^{-n}} \tag{18}$$

where y and y_0 are the fraction of bound ligand in the presence and absence of unlabeled competitor granisetron, and IC_{50} is the concentration of competing ligand that reduced y_0 by 50%. The dissociation constant of granisetron, K_i, was estimated according to Cheng and Prusoff *(31)*:

$$K_i = \frac{IC_{50}}{1 + [L]/K_d} \tag{19}$$

where [L] and K_d are the concentration and the dissociation constant of the labeled ligand, respectively.

Radioligand Binding Assays. The concentration of receptor ligand-binding sites was determined by incubation of samples containing approximately 0.2 pmol of $5HT_3$ receptor for 30 min at room temperature in buffer 2 with six concentrations of [^{3}H]GR65630, ranging from 0.1 to 40 nM in a final volume of 1 mL. The incubation was terminated by rapid filtration through Whatman GF/B filters [presoaked for 15 min in 0.5% (w/v) polyethylenimine] followed by two washes with 3 mL of ice-cold buffer 1. Filters were transferred into scintillation vials, and 4 mL of Ultima Gold (Packard, Downers Grove, IL) was added. The radioactivity was measured in a Tri-Carb 2200CA liquid scintillation counter (Packard) and corrected for quenching and counting efficiency. Nonspecific binding was determined in the presence of 1 μM quipazine. All experiments were performed in triplicate.

The dissociation constant K_d of [^{3}H]GR65630, the total concentration of $5HT_3$ receptor (expressed as concentration of binding sites), and Hill coefficients n were evaluated by fitting experimental data with the following binding isotherm:

$$[\mathrm{GR65630}]_{\mathrm{bound}} = \frac{[5\mathrm{HT}_{3\mathrm{As}}\mathrm{receptor}]_{\mathrm{total}}}{1 + (K_{\mathrm{d}}/[\mathrm{GR65630}]_{\mathrm{free}})} \quad (20)$$

The binding affinity of the receptor to the different fluorescently labeled GR compounds and to granisetron was determined by competition binding assays. Samples containing 0.2 pmol of $5HT_3$ receptor, 0.8 nM [^{3}H]GR65630 in 10 mM HEPES, 0.4 mM $C_{12}E_9$ (pH 7.4), and increasing concentrations of the competitors in a final volume of 1 mL were incubated for 30 min at room temperature. Binding inhibition curves were evaluated as above.

Steady-State Fluorescence Measurements. Fluorescence measurements were performed on a Spex Fluorolog II (Instruments S.A., Stanmore, U.K.) with 1.0 and 1.35 nm band-passes for excitation and emission, respectively. Quartz cuvettes of $10 \times 4 \times 25$ mm^3 (Hellma, Müllheim, Germany) were placed in a cell holder thermostated at 20 °C and were continuously stirred with a magnetic bar.

The effect of ligand partitioning into detergent micelles and of binding to $5HT_3$ receptor on the fluorescence intensity of the fluorescently labeled GR compounds was determined as follows. Typically, 2 nM solutions of ligand in 10 mM HEPES (pH 7.4) without or with 0.4 mM $C_{12}E_9$ were prepared, and the fluorescence excitation and emission spectra were recorded. Then, to ensure quantitative binding of the ligands, saturating concentrations of $5HT_3$ receptor (up to 40 nM) were added to the detergent solution. After having reached a final stable fluorescence intensity, spectra were acquired again. Possible fluorescence changes arising from nonspecific interactions of the GR compounds were determined by preincubating the $5HT_3$ receptor with 1 μM of the nonfluorescent ligand quipazine before its addition to the fluorescent ligand. All experiments were performed at least twice.

RESULTS

Radioligand Binding Assays. The affinity of the fluorescently labeled GR compounds for the purified His-tagged $5HT_3$ receptor, solubilized in detergent, was determined by a competition binding assay using the radioligand [^{3}H]-GR65630, which strongly binds to the receptor with a K_d of 0.24 nM and a Hill coefficient of unity *(27)*. Upon increasing the concentration of fluorescent ligands in the assays, the binding of [^{3}H]GR65630 to the $5HT_3$ receptor decreased in a monophasic manner characterized by Hill coefficients close to unity. The dissociation constants obtained for GR−NBD, GR−Flu, and GR−Rho (Table 2) increased only slightly compared to the parent compound GR-H, which exhibited a dissociation constant of 0.12 nM. However, GR−Cy5 displayed a strongly diminished affinity for the $5HT_3$ receptor (K_d = 18 nM). These data indicate that modification of GR-H on its free amino group in itself did not interfere with receptor binding, but that the nature of the fluorophore used for modification can strongly influence this process.

Steady-State Fluorescence Measurements. A crucial parameter in the evaluation of multicomponent ACFs is the relative fluorescence of all the species involved (eq 5). In our case, the fluorescent ligands can be found in three different environments: free in buffer, partitioned into micelles, and bound to the receptor. Therefore, steady-state fluorescence measurements were performed to compare the relative fluorescence of the fluorescent GR ligands under the different conditions.

Table 2: Experimentally Determined Masses and Dissociation Constants

ligand	M_{C12E9}[a] (kDa)	$M_{5\,HT3}$[a] (kDa)	K_d^{FCS}[c] (nM)	K_d^{RBA}[d] (nM)
R18	72 ± 15			
GR−NBD		652 ± 662	0.52 ± 0.77	0.5 ± 0.2
GR−Flu	230 ± 75	687 ± 1043	0.51 ± 0.24	0.32 ± 0.19
GR−Rho	74 ± 18	701 ± 383		0.8 ± 0.2
GR−Cy5	74 ± 33	486 ± 296	15.7 ± 8.0	18.0 ± 2.0

[a] M_{C12E9} is the relative molecular mass of the $C_{12}E_9$ micelles determined by FCS. [b] M_{5HT3} is the relative molecular mass of the $5HT_{3As}$ receptor in micelles determined by FCS. [c] K_d^{FCS} is the K_d determined by FCS. [d] K_d^{RBA} is the K_d determined by radioligand binding assay.

The fluorescence intensities observed for the labeled ligands with Rho 6G, fluorescein, and Cy5 were unaffected by the addition of detergent. GR−NBD was hardly detectable without detergent present. However, binding to the receptor caused significant changes: the fluorescence intensities of GR−NBD and GR−Flu decreased upon receptor binding (by 50% and 70%, respectively), whereas the fluorescence of GR−Cy5 remained unaffected, and for GR−Rho the fluorescence intensity increased by 25%.

FCS Measurements: (A) Calibration. For excitation at 488 and 514.5 nm, the FCS instrument was calibrated with Rho 6G or carboxyfluorescein. The diffusion coefficient of carboxyfluorescein was determined to be $(3.1 \pm 0.4) \times 10^{-6}$ cm^2 s^{-1} (eq 12). The diffusion coefficient of the $C_{12}E_9$ micelles was measured by FCS of R18 incorporated into the micelles to $(5.3 \pm 0.4) \times 10^{-7}$ cm^2 s^{-1}. This corresponds to an average micellar mass of 72 ± 15 kDa (eq 11). For the mass calibration of the measurements at 633 nm we used GR−Cy5 directly. All other measurements regarding relative molecular mass values were based on calibration with GR−Cy5. The experimental structure parameter K was measured to be 5 for all experimental arrangements and was held constant for all experiments.

Control experiments with fluorescein were conducted to determine the influence of evaporation on the binding experiments during the measurement time. All results were corrected with a value of 5% evaporation during 10 min of measurement for a 50 μL droplet. This value is correct for the first 30 min of measurement, and then the rate of evaporation starts to increase strongly.

The counts per fluorescent particle (cpp) were strongly dependent on the fluorophore (Figure 1). The highest cpp was reached for GR−Cy5 with 120 kHz (laser power 7 mW). For GR−Rho we obtained 10 kHz (54 kHz for Rho 6G), for GR−Flu 8 kHz, and for GR−NBD 2.5 kHz (laser power 60−80 μW). The lifetime of the triplets was 2−3 μs for GR−Flu, and 1.2−2.5 μs for GR−Cy5; for GR−NBD and GR−Rho no triplet at the applied excitation power was detected. GR−NBD was only observable in buffer 2, i.e., in the presence of detergent. In polar media like water (buffer 1) the fluorescence of the NBD-labeled ligand was too low to be detectable. All other fluorophores showed no change in fluorescence yield when incorporated into micelles (see steady-state fluorescence). The mass of the $C_{12}E_9$ micelles was determined (see Table 2) with the differently labeled ligands and the partitioning into the micelles was measured

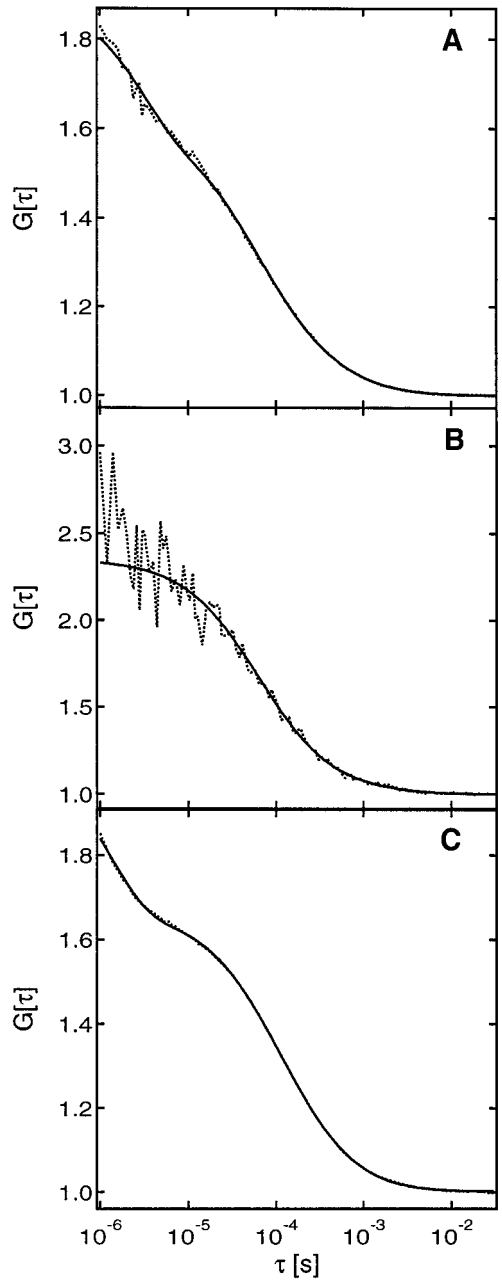

FIGURE 1: Experimental (dotted lines) and fitted (solid lines) autocorrelation functions $G(\tau)$ for the different labeled ligands in 10 mM HEPES (pH = 7.4) and $C_{12}E_9$ (0.4 mM). (A) GR−Flu delivers a count rate of 8 kHz/molecule. A triplet state can be seen at short correlation times with a lifetime of 2−3 μs. (B) GR−NBD has a count rate of 2.5 kHz/molecule. (C) GR−Cy5 yields a count rate per particle of 120 kHz; the triplet lifetime is 1.2−2.5 μs.

(GR−Flu, 16%; GR−NBD, 10%; GR−Rho, 57%; GR−Cy5, 13%).

Because GR−NBD could not be observed in polar media we used its calculated correlation time (eqs 10 and 12) for all further fits. In buffer 2 without receptor the two-component model yielded fits with $\chi_\nu^2 \approx 1$. Three-component models resulted in fits with $\chi_\nu^2 \approx 0.8$, where the third component contributed 17.7% ± 8% and had a correlation time of 800 μs (the two shorter correlation times were fixed to 67 and 344 μs, representing the ligand dissolved in water and incorporated into micelles, respectively).

(B) Stoichiometry of Ligand Binding. To determine whether the stoichiometry of ligand−receptor interaction can principally be measured by FCS, we first investigated the well-characterized binding of fluorescein-labeled biotin to streptavidin. The number of counted fluorescent particles decreased to a quarter of its initial value after several titration steps and then stayed constant independent of further addition of streptavidin, reflecting the ability of streptavidin to bind four biotin molecules (Figure 6). This experiment showed that a change of 25−50% in the number of particles can easily be observed by FCS.

To investigate the stoichiometry of ligand binding to the receptor we monitored the number of fluorescent particles in solution as dependent on the $5HT_{3As}$ receptor concentration. For GR−NBD and GR−Rho, the interpretation of the data was not unambiguous due to a low signal-to-noise ratio or aggregation, respectively.

Nevertheless, no change in the number of particles was seen for GR−Flu and GR−Cy5 upon addition of receptor. These data clearly show that only one fluorescent ligand binds per receptor homopentamer.

(C) Receptor−Ligand Affinities. For all four ligands the ACT of the ligand-containing solution increased upon the addition of $5HT_{3As}$ receptor and with increasing concentration of the receptor (GR−Flu, 69.6−84.7 μs; GR−NBD, 76.7−120.8 μs; GR−Rho, 236.8−324.3 μs; and GR−Cy5, 112.4−311.5 μs). The three-component fits resulted in dissociation constants for the interaction of the fluorescent GR compounds with the $5HT_{3As}$ receptor between 0.51 and 15.7 nM (see Table 2 and Figure 4), with the exception of GR−Rho. For GR−Rho a large number of aggregates was observed in at least 30% of the measurements (Figure 2), and dissociation constants could not be measured reliably. The ligand concentrations were between 1 and 2 nM for all ligands while the receptor concentration was varied between 0.05 nM and 1 nM for GR−Flu, GR−NBD, and GR−Rho, and between 0.9 and 35.2 nM for GR−Cy5. All models took into account the change of the fluorescence yield of the fluorophores upon binding to the receptor.

(D) Competition Measurement with the Antagonist Granisetron. The affinity of the nonfluorescent receptor antagonist granisetron was determined by a competition experiment (Figure 5). The GR−Flu concentration was 1.8 nM and the receptor concentration was 2.6 nM. The binding at this receptor ligand concentration was set to 100%. After titration of granisetron to the solution up to concentrations of 3.5 μM, the binding diminished to 19% of its initial value. The ACT decreased from 210.2 to 108.6 μs, exhibiting the same functional behavior as the binding curve. The IC_{50} was calculated to 10.9 ± 6.6 nM with a Hill coefficient of 0.61 ± 0.25.

(E) Mass Determination of the Receptor by FCS. For all ligands we calculated the average molecular mass of the receptor detergent complex from the slowest correlation time in the three-component fits (see Table 2). While for GR−Cy5 the correlation time for the third component had comparable errors for all measurements independent of the amount of receptor bound, this was not the case for the other three fluorophores. For GR−Flu and GR−NBD we calculated the molecular mass from the measurements with the highest percentage of bound receptor. For GR−Rho only those measurements were considered where no aggregates were observed. Because the mass depends on the third power of the correlation time (eq 11), the relative error in the

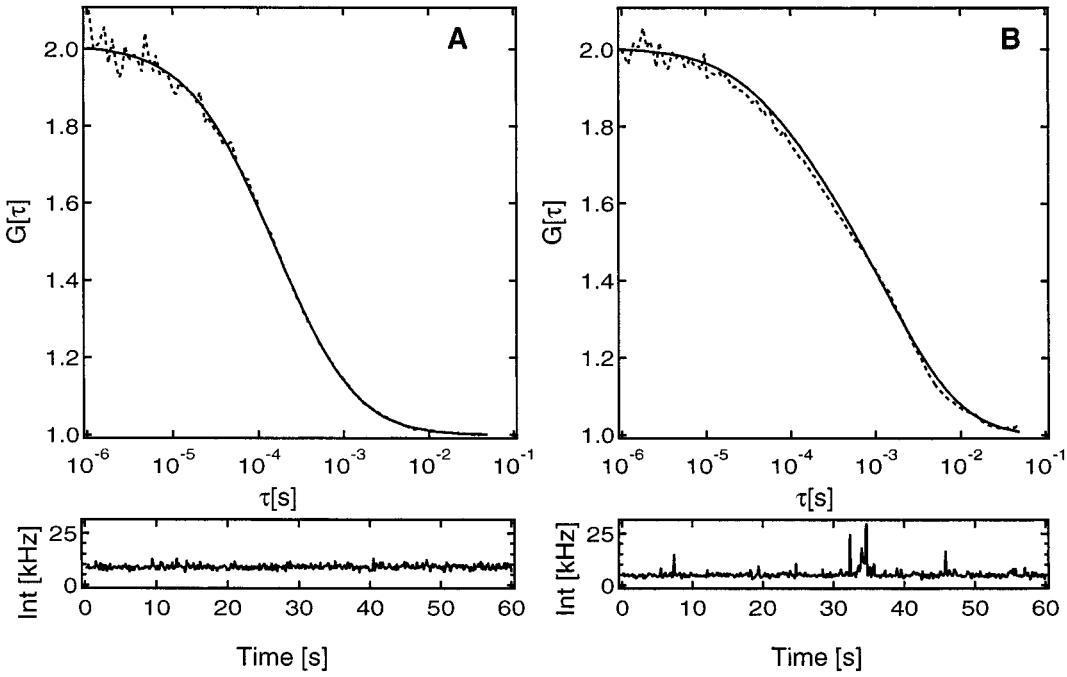

FIGURE 2: Correlation functions (top panels; dotted line shows experimental ACF, solid line shows fit) and fluorescence intensity signals (bottom panels) of GR−Rho. (A) GR−Rho in buffer 2. The ACF can be fitted with a model assuming two particles in solution (GR−Rho and GR−Rho partitioned into $C_{12}E_3$ micelles); the intensity signal is smooth, and no aggregates are visible. (B) GR−Rho in buffer 2 in the presence of $5HT_{3As}$ receptor. Large peaks can be seen in the intensity signal, probably due to aggregates of receptor/micelles and GR−Rho. A two- or three-particle model cannot adequately fit the ACF.

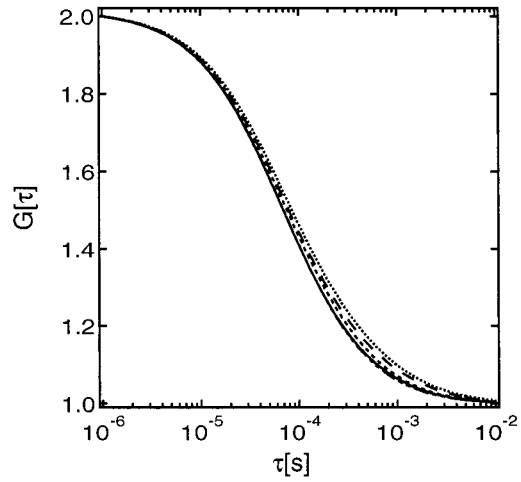

FIGURE 3: One-component fits to the experimental ACFs (experimental data not shown) for GR−NBD (1.0−1.2 nM) with increasing concentrations of $5HT_{3As}$ receptor. The measurements were performed in buffer 2. All fit functions were normalized for clarity. The average correlation time increased with the receptor concentration: 75.0 μs (0.0 nM, —) to 76.2 μs (0.05 nM, -•••-), 84.9 μs (0.11 nM, - - -), 103.6 μs (0.25 nM, — — —), and 120.8 μs (0.46 nM, ...), respectively.

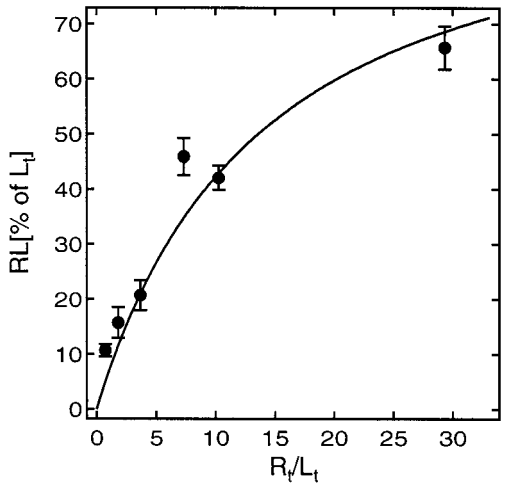

FIGURE 4: Binding of the ligand GR−Cy5 to the $5HT_{3As}$ receptor. Solutions with a concentration of 1.2 nM GR−Cy5 and receptor concentrations between 0.9 and 35.2 nM were prepared. The concentration of the ligand−receptor complex RL obtained from the individual ACFs is plotted versus the ratio of total receptor and total ligand (R_t/L_t). The experimental data were fitted to a binding isotherm (eq 17), yielding a dissociation constant of $K_d = 15.7 \pm 8.0$ nM.

correlation time causes a three times larger relative error in the mass. The relative molecular mass determined ranges from 486 to 701 kDa with relative errors between 55% and 152%.

DISCUSSION

The antagonistic ligand GR-119566X for the $5HT_{3As}$ receptor was labeled with one of four different fluorophores to measure the binding of the thus produced fluorescent ligands to the receptor by FCS. All labeled ligands showed binding but the affinity depended on the particular fluorophore. The affinities measured by FCS and radioligand assays agreed very well (Table 2). This shows that all four labels are generally suited for FCS measurements.

Fluorescein delivered high count rates per molecule and gives reliable answers whether binding occurred. This could be seen in both the fraction of ligand bound in the two-component fit and the corresponding ACT in the one-component fit to the FCS data. However, the mass determination for micelles and for the receptor protein showed high errors and differed from that of the other fluorophores (see below). This is probably due to the high number of

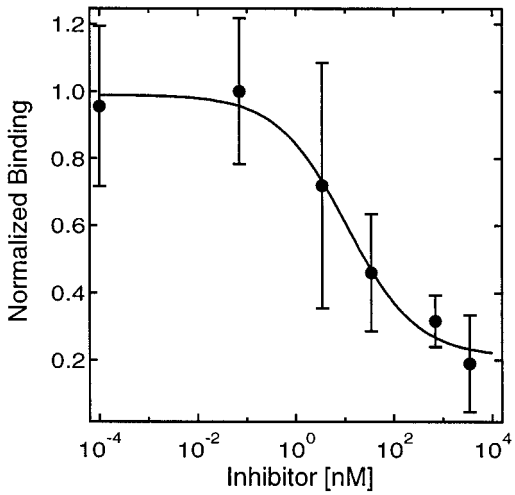

FIGURE 5: Competitive inhibition of granisetron for the binding of GR−Flu to the $5HT_{3As}$ receptor. The concentration of granisetron was varied between 0.1 pM and 3.5 μM. The binding data were fitted to a binding isotherm (solid line), yielding an $IC_{50} = 10.9 \pm 6.6$ nM and a Hill coefficient of 0.61 ± 0.25. All measurements were done in buffer 2. The $5HT_{3As}$ receptor and GR−Flu concentrations were 8.8 and 1.75 nM, respectively.

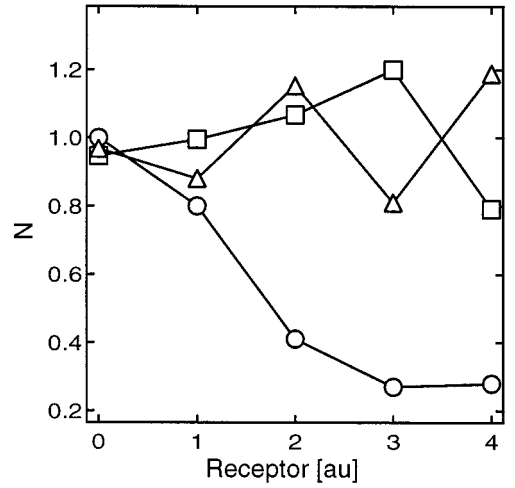

FIGURE 6: Determination of the stoichiometry of ligand binding to the $5HT_{3As}$ receptor. The concentration of fluorescent particles was measured for samples of GR−Flu or GR−Cy5 with increasing concentrations of $5HT_{3As}$ receptor. For GR−Flu (□), the concentration of the ligand varied from 1.9 to 1.5 nM, the receptor concentration increased from 0.0 to 0.85 nM, and concomitantly the ligand binding increased from 0 to 40% of total ligand concentration. Relative errors are smaller than 15% for all measurements. In the case of GR−Cy5 (△), the ligand was held constant at 1.2 nM, and the receptor concentration varied from 0.0 to 35.2 nM, with a concomitant increase of ligand binding from 0.0 to 65.7% of total ligand concentration. Relative errors are smaller than 3% for all points. No significant decrease of the particle number of the fluorescent ligands was observed. In a control experiment (○), biotin−fluorescein (3.6 nM) was titrated with increasing concentrations of streptavidin (0−1.8 nM), resulting approximately in a 4-fold decrease of the number of fluorescent particles in solution at 0.9 nM streptavidin. The relative error was in the range of 20%. For GR−Flu and biotin−fluorescein the number of particles is corrected for changing ligand concentrations during titration. The abscissa shows the number of titration steps, with increasing receptor concentration from left to right. All data points are an average of 10 experiments. All curves were normalized to their maximum value. Error bars were omitted for clarity.

molecules in the triplet state whose fraction and lifetime change with the local environment *(32)*. Because the triplet fraction and lifetime of fluorescein was a free parameter in the fits it might be partially correlated with the diffusion time and thus yield a higher spread in the measurement. Nonetheless, keeping the triplet parameters constant did result in higher values of χ^2.

NBD is a fluorophore with a low relative molecular mass (200 Da) and is therefore a good candidate if small ligands that enter a narrow binding pocket of a receptor have to be labeled without disturbing molecular interactions. Unfortunately, because of its low fluorescence intensity in polar media the diffusion time of GR−NBD cannot be measured in pure water. When detergent is added, the fluorescence yield of GR−NBD increases but the experimental data can only be fitted with two components. We calculated in these measurements the theoretical diffusion times with the Stokes−Einstein equation (eq 7) and kept these values constant in all measurements. Because of the low number of photons emitted per molecule, the noise in the GR−NBD measurements is higher than for the other fluorophores. This low signal-to-noise ratio is especially dominant at very short correlation times, where only a low number of photons are measured per channel (the probability that a photon is found in a channel is about 5×10^{-4}), and at very long correlation times, where only a small number of measurements is performed because of the longer measurement time per channel (this is an effect of the semilogarithmic time scale used by the hardware correlator, which ranges from 0.2 μs for small correlation times up to seconds for the longer correlation times). Consequently, it is difficult to obtain good fits for longer diffusion times and a third component with a correlation time in the millisecond range can be seen without the addition of receptor. This fraction was $17.7\% \pm 8.0\%$. We subtracted this background from all other measurements. Nonetheless, the binding of receptor can be easily detected when the ACT is measured (Table 2 and Figure 3) even when NBD has only a very low fluorescence yield.

Both Rho 6G and Cy5 gave high count rates per molecule and were very photostable. The GR ligands labeled with these compounds showed in all measurements a clear shift of the ACT when receptor was added. A difference in the amount of binding of less than 5% between two samples was easily detected. The determination of masses for micelles and the receptor showed errors of "only " 50−60%, which is much better than the other fluorophores. But both fluorophores have disadvantages if one wants to measure binding constants.

GR−Rho interacted with surfaces and was therefore depleted in solution, making absolute measurements unreliable. In addition, the ligand−protein complexes showed a strong tendency to aggregate, reflected by the distinct fluorescent peaks appearing in about 30% of the measurements in the average fluorescence intensity. These peaks stem from aggregates of labeled ligands and/or receptor proteins (Figure 2), showing correlation times above 1 ms. If such measurements were excluded from the evaluation, the mass determination agreed very well with those obtained from the other fluorophores.

Cy5 has a relative molecular mass of 791 Da and is thus large compared to the functional, unlabeled ligand of 336 Da. It is therefore possible that the decrease in receptor binding affinity of GR−Cy5 of almost 2 orders of magnitude in comparison with the unlabeled ligand might be due to steric hindrance of the fluorophore. On the other hand, the

high count rate per molecule attainable with GR−Cy5 resulted in a low signal-to-noise ratio and made mass determinations already reliable when only a small amount of protein was bound. For GR−Rho and GR−Cy5 we used long measurement times of 60 and 30 s, respectively, to increase the accuracy of the measurement *(29)*. But because of the high count rates per molecule obtained for both fluorophores, measuring times could be reduced to the order of 1−10 s if only a "yes or no answer" for binding is desired.

From these results we can conclude that to choose a suitable ligand for FCS measurements one has to weigh between the higher accuracy of a high count rate fluorophore and the presumed disturbance of the ligand−receptor interaction by this label. Because the fluorophores presented here cover a wide range in the electromagnetic spectrum they can be selected according to the necessities of the measurement and the influence they have on the molecular interactions.

In general, accurate mass determinations are difficult to perform by FCS because the correlation time depends on the cubic root of the mass (eq 11). Aggregation can further distort the results as in the case of GR−Rho. The mass of the $C_{12}E_9$ micelles was determined using R18, which incorporated completely in micelles; only one diffusion time could be observed in the ACFs, from which an average mass of 72 ± 15 kDa for a micelle was evaluated. The aggregation number of $C_{12}E_9$ is not reported in the literature, but for the related detergent $C_{12}E_8$ [octa(ethylene glycol) monododecyl ether], an aggregation number of 120−123, and thus an average relative micellar mass of 66 kDa per micelle, is published *(33, 34)*. Assuming a similar aggregation number for $C_{12}E_9$ yields a relative micellar mass of 72 kDa. This is in excellent agreement with our FCS results and this was further confirmed by the measurements on GR−Rho and GR−Cy5 (both yielded 74 kDa), although they showed a much lower partitioning into the micelles than R18.

The relative micellar mass of the $5HT_{3As}$ receptor/detergent complex determined here by FCS ranges between 486 and 701 kDa with relative errors between 55% and 152% (see Table 2). This is in agreement with reported data ranging between 250 and 670 kDa *(14, 27, 35−37)*. The estimated relative molecular mass of the receptor (based on its amino acid sequence) plus the contribution from the micelle is about 320 kDa.

When a high percentage of ligand is bound and thus the ligand−receptor complex contributes substantially to the fluorescence signal, the mass determination is fairly accurate with errors between 50% and 150%. In cases where only a small fraction of the ligand is bound, the ligand−receptor complex contributes only little to the fluorescence signal and errors can be as high as 300%. Nonetheless, even in the worst case, FCS gives the right order of magnitude for relative molecular masses and compares favorably with other techniques such as gel filtration or analytical ultracentrifugation.

The above-mentioned relative molecular masses calculated from the ACFs of FCS experiments are based on two assumptions: first, that the fluorophores used for both the calibration and the receptor−detergent complex adopt a spherical shape, and second, that these putative spheres all have the same specific density. In electron microscopic images the $5HT_{3As}$ receptor showed an elongated, cylindrical shape similar to that of the nACh receptor *(37, 38)*. The correlation time for such a structure is expected to be higher than for a sphere *(39)*, and therefore the actual molecular masses of the receptor−detergent complex should be distinctly lower than estimated for the spherical case.

Competition ligand binding experiments between fluorescent and nonfluorescent compounds are equally feasible by FCS as demonstrated for the couple GR−Flu and the nonfluorescent antagonist granisetron. Values of 10.9 ± 6.6 nM for the IC_{50} and 0.61 ± 0.25 for the Hill coefficient are in good agreement with recently published data *(16)*.

Both GR−Flu and GR−Cy5 bind with a 1:1 stoichiometry to the $5HT_{3As}$ receptor. The results for GR−Rho and GR−NBD were unreliable because of unspecific binding and aggregation or low signal-to-noise ratio, respectively. The 1:1 ligand−receptor stoichiometry is directly reflected by the number of fluorescent particles, which did not change upon addition of receptor (Figure 6); a significant decrease in particle number would be expected if more than one ligand bound per receptor. Moreover, all binding curves could be fitted accurately by Langmuir isotherms, which assumes independent binding sites on the receptor molecule. A 1:1 stoichiometry was also deduced from an analysis of the kinetics of GR−Flu binding to the purified $5TH_3$−R *(16)* and is corroborated by the specific radioligand binding of the receptor *(27)*. In contrast, the homopentameric α_7 acetylcholine receptor, which shares a 30% sequence homology with the $5HT_{3As}$ receptor, seems to bind 5 molecules of the antagonist methyllycaconitine per receptor as deduced by modeling of the kinetics of the recovery of inhibition, although binding of one methyllycaconitine was already sufficient to inhibit the channel *(40)*.

However, it cannot be excluded that the GR−ligands are allosteric inhibitors. In this case one molecule might bind to an allosteric site near the symmetry axis and stabilize the receptor in an inactive state with low affinity for other ligands. This explanation would avoid the apparent contradiction of the 1:1 stoichiometry of the binding of these ligands to a homopentameric receptor. The distinction whether GR−ligands are competitive antagonists or allosteric inhibitors deserves further investigation and will be followed up by additional experiments.

As a conclusion of the present work we emphasize two major points. First, FCS is a suitable method to characterize in detail the interaction between ligands and their membrane protein receptors. In this context it is of particular importance that the stoichiometry of the ligand receptor complex can be determined in a model-free approach. This was demonstrated for the example of the $5HT_{3As}$ receptor which binds only one antagonist (GR-119566X). Second, it has been shown that fluorescent labels influence FCS measurements either by their photophysical properties, and thus have a direct impact on the quality and the necessary length of the measurement, or by their chemical properties, influencing the interaction between molecules. Thus the choice of one or several fluorophores, which are needed for a characterization of a ligand receptor system, is important and has to be adapted to the particular problem.

FCS is gaining more and more importance as a tool in biophysics and biochemistry. Its ability to measure concentrations and diffusion coefficients gives direct access to chemical and biological interactions and processes. New information can be obtained on the stoichiometry of ligand−receptor interactions and biochemical processes can be

monitored, e.g., polymerase chain reaction (PCR) *(41)*, conformational changes of DNA *(42)*, and enzymatic activity *(43)*. Because of its small observation volume, the amount of substance needed is minute and thus this technique will be a very useful tool in further characterization of molecular interactions, especially for receptors that are available in only small quantities.

ACKNOWLEDGMENT

We thank Daniel Müller for his contribution to the experiments with GR-Cy5. Horst Blasey (Serono Pharmaceutical Research Institute S.A., Chemin des Aulx 14, CH-1228 Plan-les-Ouates, Geneva, Switzerland) and Kenneth Lundström (F. Hoffmann-La Roche, Research Laboratories, CH-4070 Basel, Switzerland) are acknowledged for the large-scale expression of the $5HT_{3As}$ receptor. We also thank an anonymous reviewer for pointing out that the GR−ligands might be allosteric inhibitors.

REFERENCES

1. Ehrenberg, M., and Rigler, R. (1974) *Chem. Phys. 4*, 390−401.
2. Ehrenberg, M., and Rigler, R. (1976) *Q. Rev. Biophys. 9*, 69−81.
3. Elson, E. L., and Madge, D. (1974) *Biopolym. 13*, 1−27.
4. Madge, D., Elson, E. L., and Webb, W. W. (1974) *Biopolymers 13*, 1−27.
5. Eigen, M., and Rigler, R. (1994) *Proc. Natl. Acad. Sci. U.S.A. 91*, 5740−5747.
6. Edelstein, J., Schaad, O., and Changeux, J.-P. (1997) *Biochemistry 36*, 13755−13760.
7. Rigler, R., Widengren, J., and Mets, Ü. (1992) in *Fluorescence spectroscopy* (Wolfbeis, O. S., Ed.) pp 13−24, Springer-Verlag, Berlin, Heidelberg, and New York.
8. Thompson, N. L. (1991) in *Topics in fluorescence spectroscopy, Volume 1: Techniques* (Lakowicz, J. R., Ed.) pp 337−378, Plenum Press, New York.
9. Widengren, J. (1996) Fluorescence Correlation Spectroscopy, Photophysical Aspects and Applications, Ph.D. Thesis, Department of Medical Biophysics, Karolinska Institute, Stockholm, Sweden.
10. Haupts, U., Maiti, S., Schwille, P., and Webb, W. W. (1998) *Proc. Natl. Acad. Sci. U.S.A. 95*, 13573−13578.
11. Rauer, B., Neumann, E., Widengren, J., and Rigler, R. (1996) *Biophys. Chem. 58*, 3−12.
12. Klingler, J., and Friedrich, T. (1997) *Biophys. J. 73*, 2195−2200.
13. Knowles, J. (1997) *Curr. Opin. Biotechnol. 8*, 667−668.
14. Hamon, M. (1992) in *Neuroscience Perspectives* (Jenner, P., Ed.) Academic Press Ltd., London.
15. Schmid, E. L., Tairi, A.-P., Hovius, R., and Vogel, H. (1998) *Anal. Chem. 70*, 1331−1338.
16. Tairi, A.-P., Hovius, R., Pick, H., Blasey, H., Bernard, A., Surprenant, A., Lundström, K., and Vogel, H. (1998) *Biochemistry 37*, 15850−15864.
17. Unwin, N. (1993) *Cell/Neuron 72*, 31−41.
18. Edelstein, S. J., and Bardsley, W. G. (1997) *J. Mol. Biol. 267*, 10−16.
19. Davies, A., Pistis, M., Hanna, M., Peters, J., Lambert, J., Hales, T., and Kirkness, E. (1999) *Nature 397*, 359−363.
20. Aragon, S. R., and Pecora, R. (1976) *J. Chem. Phys. 64*, 1791−1803.
21. Rigler, R., Mets, U., Widengren, J., and Kask, P. (1993) *Eur. Biophys. J. 22*, 169−175.
22. Widengren, J., Rigler, R., and Mets, Ü. (1994) *J. Fluoresc. 4*, 255−258.
23. Widengren, J., Mets, Ü., and Rigler, R. (1995) *J. Phys. Chem. 99*, 13368−13379.
24. Chandrasekhar, S. (1943) *Rev. Mod. Phys. 15*, 1−89.
25. Clegg, R. M., and Vaz, W. L. C. (1985) in *Progress in Protein−Lipid Interactions* (Watts, A., and DePont, J. J. H. H. M., Eds.) pp 173−229, Elsvier Science, Amsterdam.
26. Lundström, K., Michel, A., Blasey, H., Bernard, A. R., Hovius, R., Vogel, H., and Surprenant, A. (1997) *J. Recept. Signal Transduct. Res. 17*, 115−126.
27. Hovius, R., Tairi, A.-P., Blasey, H., Bernard, A., Lundström, K., and Vogel, H. (1998) *J. Neurochem. 70*, 824−834.
28. Saleh, B. E. A., and Teich, M. C. (1991) *Fundamentals of Photonics*, John Wiley & Sons, Inc., New York.
29. Koppel, D. E. (1974) *Phys. Rev. A 10*, 1938−1945.
30. Meseth, U., Wohland, T., and Vogel, H. (1999) *Biophys. J. 76*, 1619−1631.
31. Cheng, Y. C., and Prusoff, W. H. (1973) *Biochem. Pharmacol. 22*, 3099−3108.
32. Song, L., Varma, C. A., Verhoeven, J. W., and Tanke, H. J. (1996) *Biophys. J. 70*, 2959−2968.
33. Bhairi, S. M. (1997) *Detergents*, Calbiochem-Novabiochem Corporation, La Jolla, CA.
34. Tanford, C., Nozaki, Y., and Rohde, M. F. (1977) *J. Phys. Chem. 81*, 1555−1560.
35. Gordon, J. C., Sarbin, N. S., Barefoot, D. S., and Pinkus, L. M. (1990) *Eur. J. Pharmacol. 188*, 313−319.
36. McKernan, R. M., Biggs, C. S., Gillard, N., Quirk, K., and Ragan, C. I. (1990) *Biochem. J. 269*, 623−628.
37. Boess, F. G., Beroukhim, R., and Martin, I. L. (1995) *J. Neurochem. 64*, 1401−1405.
38. Unwin, N. (1993) *J. Mol. Biol. 229*, 1101−1124.
39. Elias, H. G. (1984) *Macromolecules*, 2nd ed., Plenum Press, New York.
40. Palma, E., Bertrand, S., Binzoni, T., and Bertrand, D. (1996) *J. Physiol. 491*, 151−161.
41. Walter, N. G., Schwille, P., and Eigen, M. (1996) *Proc. Natl. Acad. Sci. U.S.A. 93*, 12805−12810.
42. Bonnet, G., Krichevsky, O., and Libchaber, A. (1998) *Proc. Natl. Acad. Sci. U.S.A. 95*, 8602−8606.
43. Kinjo, M., Nishimura, G., Koyoma, T., Mets, Ü., and Rigler, R. (1998) *Anal. Biochem. 260*, 166−172.

BI990366S